of the interior. Chapter headings include the internal constitution of the earth, gravity field, gravity potential, equilibrium figure, gravity measurements, reduction of gravity measurements, isostasy, gravity anomalies, physical geodesy, deviations from isostasy, and convection currents in the earth.

Kaula, W. M., *An Introduction to Planetary Physics* (John Wiley & Sons, New York, 1968), 490 pages. A basic textbook on planetary physics for graduate students. While several chapters deal with aspects of the earth's interior, the emphasis is on all the terrestrial planets. In addition to the standard topics such as gravity, seismology, and magnetism, there are chapters on the dynamics of the earth-moon system, the dynamics of the solar system, the geology of the moon and Mars, remote sensing of the planets, meteorites, and planetary origins. Each chapter contains problems for the student.

Phillips, R. J., and K. Lambeck, Gravity fields of the terrestrial planets: long-wavelength anomalies and tectonics, *Reviews of Geophysics and Space Physics, vol. 18*, pages 27–76, 1980. A review paper on the long-wavelength gravity fields of the terrestrial planets earth, Moon, Mars, and Venus. Emphasis is placed on the implications of gravity anomalies for the interior mechanical properties and states of stress of the planets.

Pick, M., J. Picha, and V. Vyskocil, *Theory of the Earth's Gravity Field* (Elsevier Scientific Publishing Company, Amsterdam, 1973), 538 pages. A fundamental textbook on gravimetry for graduate students in solid earth geophysics and geodesy. The coverage of the subject is extensive and includes potential theory, relative measurements of the acceleration of gravity, gravity anomalies and their interpretations, gravimetry and the earth's internal structure, the geoid, the earth's figure, tides, and astronomical aspects. There is a lengthy appendix on the mathematical techniques employed in the book.

Stacey, F. D., *Physics of the Earth* (John Wiley & Sons, New York, 1977), 414 pages. A fundamental textbook on geophysics for graduate and advanced undergraduate students. Topics covered include the earth as a part of the solar system, radioactivity and the age of the earth, the earth's rotation, gravity, tides, seismology, the earth's internal heat, geomagnetism, paleomagnetism, and tectonics. There are tables of useful data and appendices on special topics and problems for the student.

chapter 6

FLUID MECHANICS

6-1 INTRODUCTION

Any material that flows in response to an applied stress is a *fluid*. Although solids acquire a finite deformation or strain upon being stressed, fluids deform continuously under the action of applied forces. In solids, stresses are related to strains; in fluids, stresses are related to *rates of strain*. Strains in solids are a consequence of spatial variations or gradients in the displacements of elements from their equilibrium positions. Strain rates in fluids are a result of gradients in the velocities or rates of displacement of fluid elements. Velocity gradients are equivalent to strain rates, so that stresses in fluids are related to velocity gradients. The equation connecting stresses with velocity gradients in a fluid is known as the rheological law for the fluid. The simplest fluid, and as a consequence the one most often studied, is the *Newtonian or linear fluid*, in which the rate of strain or velocity gradient is directly proportional to the applied stress; the constant of proportionality is known as the *viscosity*. We deal only with Newtonian viscous fluids throughout this chapter. Non-Newtonian fluid behavior is discussed in Chapter 7. *Fluid mechanics* is the science of fluid motion. It uses the basic principles of *mass, momentum, and energy conservation* together with the rheological or *constitutive law* for the fluid to describe how the fluid moves under an applied force.

Many problems involving fluid mechanics arise in geodynamics. Obvious examples involve flows of groundwater and magma. Groundwater flows through underground channels known as *aquifers*. If the aquifers are sufficiently deep and pass through rock sufficiently hot, hot springs may result. In areas of active *volcanism* the groundwater may be heated above the *boiling point* and *geysers* result. In some cases steam or very hot water is trapped at depth, and these may provide *reservoirs for geothermal power plants*. The circulation of *seawater* through the *oceanic crust* is similar in many respects to the flow of groundwater on land. Seawater can become so hot in passing through crustal rocks near an oceanic ridge that *submarine hot springs* develop.

Geochemical studies show that magmas flowing from surface *volcanoes* have in some cases originated at depths of 100 km or more. Studies of extinct volcanoes show that the magma flows through *volcanic conduits* at shallow depths. In some cases these conduits have the form of near circular pipes and in other cases two-dimensional channels. Mechanisms for the flow of magma at depths of greater than about 5 km are a subject of considerable controversy. Alternative hypotheses involve propagating *fractures*, large bodies of ascending magma, and continuous conduits.

In terms of geodynamics, however, one of our principal interests is *mantle convection*. The fluid behavior of the mantle is responsible for *plate tectonics* and *continental drift*; it plays a dominant role in determining the thermal structure of the earth. An understanding of *thermal convection* is essential to the understanding of fundamental geodynamic processes. When a fluid is heated from

within or from below and cooled from above, thermal convection can occur. The hotter fluid at depth is *gravitationally unstable* with respect to the cooler fluid near the upper surface. *Buoyancy forces* drive the convective flow.

On many scales crustal rocks appear to have been folded. *Folding* can be attributed to the fluid behavior of these rocks. A fluid instability can also explain the formation of *salt domes* due to the *diapiric upwelling* of a buried layer of salt. The salt is gravitationally unstable because of its low density.

6-2 ONE-DIMENSIONAL CHANNEL FLOWS

The movement of the plates over the surface of the earth represents a flow of mantle rock from accreting plate boundaries to subduction zones. A complementary flow of mantle rock from subduction zones to accreting plate boundaries must occur at depth. One model for this counterflow assumes that it is confined to the asthenosphere immediately below the lithosphere. Interpretations of postglacial rebound data suggest the presence of a thin (of the order of 100 km thick) low-viscosity region beneath the oceanic lithosphere. In addition, seismic studies show that there is a region beneath the lithosphere in which the seismic velocities are low and the seismic waves, particularly shear waves, are attenuated. This layer, the seismic low-velocity zone, has a thickness of about 200 km. Although the presence of a seismic low-velocity zone is not direct evidence of the existence of a low-viscosity region, the physical circumstances responsible for the reduction in seismic wave speeds and the attenuation of the waves (high temperature, small amounts of partial melting) also favor the formation of a low-viscosity region. Any flow in an asthenosphere would be approximately horizontal because of the large horizontal distances involved (the dimensions of lithospheric plates are thousands of kilometers) compared with the small vertical dimension of the region. Thus we consider one-dimensional flow of a Newtonian viscous fluid in a channel between parallel plates as a model for asthenospheric flow.

Figure 6-1 is a sketch of a one-dimensional channel flow. The fluid moves with velocity u in the x direction in a channel of thickness h. The horizontal velocity varies only with the vertical coordinate; that is, $u=u(y)$, where y is the distance from the upper boundary ($y=0$). The flow may occur as a result of either an applied horizontal *pressure gradient* $(p_0-p_1)/l$ (l is the horizontal length of a section of the channel, p_1 is the pressure at the entrance to the section, and p_0 is the pressure at the section exit) or the prescribed motion of one of the walls (here it is assumed that the upper boundary $y=0$ has the given speed $u=u_0$ and the lower boundary $y=h$ is motionless). The flow may also be driven by a combination of a pressure gradient and a prescribed wall velocity. As a result of the *shear*, or gradient in the velocity profile, a *shear stress* τ (force per unit area) is exerted on horizontal planes in the fluid and at the

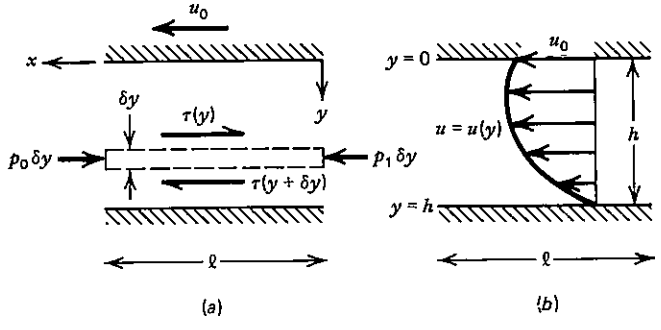

Figure 6-1 (*a*) The force balance on a layer of fluid in a channel with an applied pressure gradient. (*b*) A typical velocity profile.

channel walls. For a Newtonian fluid with constant *viscosity* μ the shear stress at any location in the channel is given by

$$\tau=\mu\frac{du}{dy} \tag{6-1}$$

The shear stress defined in Equation (6-1) is the tangential stress on a surface whose outer normal points in the y direction. The viscosity of a Newtonian fluid is the constant of proportionality between shear stress and strain rate or velocity gradient. The more viscous the fluid, the larger the stress required to produce a given shear. The viscosities of some common fluids are listed in Table 6-1. The SI unit of viscosity is the Pa s (the cgs unit is the poise, 10 poise=1 Pa s). The ratio μ/ρ (ρ is the density of the fluid) occurs frequently in fluid mechanics. It is known as the *kinematic viscosity* ν of a fluid

$$\nu=\frac{\mu}{\rho} \tag{6-2}$$

The quantity μ is the dynamic viscosity. The SI unit of kinematic viscosity is $m^2\ s^{-1}$ (the cgs unit is $cm^2\ s^{-1}$). The kinematic viscosity is a diffusivity, similar to the thermal diffusivity κ. While κ describes how heat diffuses by molecular collisions, ν describes how momentum diffuses. The ratio of ν to κ is a dimensionless quantity known as the *Prandtl number Pr*

$$Pr\equiv\frac{\nu}{\kappa} \tag{6-3}$$

A fluid with a small Prandtl number diffuses heat more rapidly than it does momentum; the reverse is true for a fluid with a large value of *Pr*. Table 6-1 also lists the kinematic viscosities, thermal diffusivities, and Prandtl numbers of a variety of fluids.

The flow in the channel in Figure 6-1 is determined by the *equation of motion*. This is a mathematical statement of the *force balance* on a layer of fluid of thickness δy and horizontal length l (see Figure 6-1). The net *pressure force* on the element in the x direction is

$$(p_1-p_0)\,\delta y$$

(this is the force per unit depth of the channel in the direction normal to the plane in Figure 6-1). Since the shear stress as well as the velocity is a function only of y, the shear force on the upper boundary of the layer in the x direction is

$$-\tau(y)l$$

and the shear force on the lower boundary of the layer in the x direction is

$$\tau(y+\delta y)l=\left(\tau(y)+\frac{d\tau}{dy}\delta y\right)l \tag{6-4}$$

The net force on the layer must be zero. This gives

$$(p_1-p_0)\delta y+\left\{\tau(y)+\frac{d\tau}{dy}\delta y\right\}l-\tau(y)l=0 \tag{6-5}$$

which in the limit $\delta y\to 0$ becomes

$$\frac{d\tau}{dy}=-\frac{(p_1-p_0)}{l} \tag{6-6}$$

Table 6-1 Transport Properties of Some Common Fluids at 15°C and Atmospheric Pressure

	Viscosity μ (Pa s)	Kinematic Viscosity ν ($m^2\ s^{-1}$)	Thermal Diffusivity κ ($m^2\ s^{-1}$)	Prandtl Number Pr
Air	1.78×10^{-5}	1.45×10^{-5}	2.02×10^{-5}	0.72
Water	1.14×10^{-3}	1.14×10^{-6}	1.40×10^{-7}	8.1
Mercury	1.58×10^{-3}	1.16×10^{-7}	4.2×10^{-6}	0.028
Ethyl alcohol	1.34×10^{-3}	1.70×10^{-6}	9.9×10^{-8}	17.2
Carbon tetrachloride	1.04×10^{-3}	6.5×10^{-7}	8.4×10^{-8}	7.7
Olive oil	0.099	1.08×10^{-4}	9.2×10^{-8}	1,170
Glycerine	2.33	1.85×10^{-3}	9.8×10^{-8}	18,880

The right side of Equation (6-6) is the horizontal pressure gradient in the channel

$$\frac{dp}{dx} = -\frac{(p_1 - p_0)}{l} \tag{6-7}$$

in terms of which the equation of motion can be written

$$\frac{d\tau}{dy} = \frac{dp}{dx} \tag{6-8}$$

With $p_1 > p_0$, a pressure difference tending to move the fluid in the positive x direction, the pressure gradient dp/dx is negative. The pressure drop in a channel is often expressed in terms of a *hydraulic head H* given by

$$H \equiv \frac{(p_1 - p_0)}{\rho g} \tag{6-9}$$

The hydraulic head is the height of fluid required to hydrostatically provide the applied pressure difference $p_1 - p_0$.

An equation for the velocity can be obtained by substituting the expression for τ from Equation (6-1) into Equation (6-8). We obtain

$$\mu \frac{d^2u}{dy^2} = \frac{dp}{dx} \tag{6-10}$$

Integration of this equation gives

$$u = \frac{1}{2\mu}\frac{dp}{dx}y^2 + c_1 y + c_2 \tag{6-11}$$

In order to evaluate the constants, we must satisfy the boundary conditions that $u = 0$ at $y = h$ and $u = u_0$ at $y = 0$. These boundary conditions are known as *no-slip boundary conditions*. A viscous fluid in contact with a solid boundary must have the same velocity as the boundary. When these boundary conditions are satisfied, Equation (6-11) becomes

$$u = \frac{1}{2\mu}\frac{dp}{dx}(y^2 - hy) - \frac{u_0 y}{h} + u_0 \tag{6-12}$$

If the applied pressure gradient is zero, $p_1 = p_0$ or $dp/dx = 0$, the solution reduces to the linear velocity profile

$$u = u_0\left(1 - \frac{y}{h}\right) \tag{6-13}$$

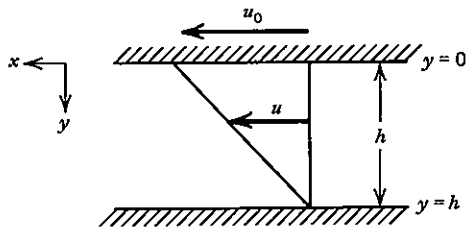

(a) Couette flow $\frac{dp}{dx} = 0, u_0 \neq 0$

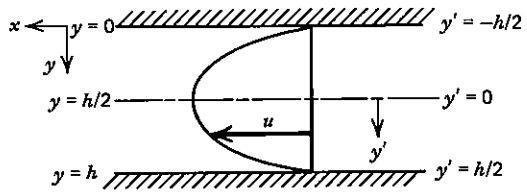

(b) $\frac{dp}{dx} \neq 0, u_0 = 0$

Figure 6-2 One-dimensional channel flows of a constant viscosity fluid.

This simple flow, sketched in Figure 6-2*a*, is known as *Couette flow*. If the velocity of the upper plate is zero, $u_0 = 0$, the velocity profile is

$$u = \frac{1}{2\mu}\frac{dp}{dx}(y^2 - hy) \tag{6-14}$$

When this is rewritten in terms of distance measured from the centerline of the channel y'

$$y' = y - \frac{h}{2} \tag{6-15}$$

one finds

$$u = \frac{1}{2\mu}\frac{dp}{dx}\left(y'^2 - \frac{h^2}{4}\right) \tag{6-16}$$

The velocity profile is a parabola that is symmetric about the centerline of the channel, as shown in Figure 6-2*b*.

Problem 6-1 Show that the mean velocity in the channel is given by

$$\bar{u} = -\frac{h^2}{12\mu}\frac{dp}{dx} + \frac{u_0}{2} \tag{6-17}$$

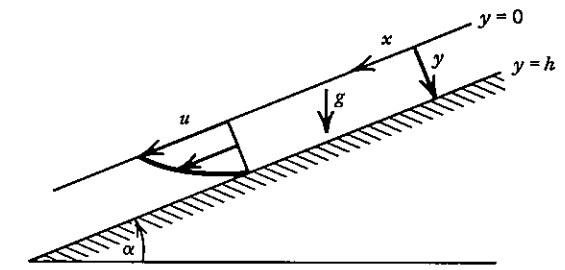

Figure 6-3 Unidirectional flow of a constant thickness layer of viscous fluid down an inclined plane.

Problem 6-2 Derive a general expression for the shear stress τ at any location y in the channel. What are the simplified forms of τ for Couette flow and for the case $u_0 = 0$?

Problem 6-3 Find the point in the channel at which the velocity is a maximum.

Problem 6-4 Consider the steady, unidirectional flow of a viscous fluid down the upper face of an inclined plane. Assume that the flow occurs in a layer of constant thickness h, as shown in Figure 6-3. Show that the velocity profile is given by

$$u = \frac{\rho g \sin\alpha}{2\mu}(h^2 - y^2) \tag{6-18}$$

where y is the coordinate measured perpendicular to the inclined plane ($y = h$ is the surface of the plane), α is the inclination of the plane to the horizontal, and g is the acceleration of gravity. First show that

$$\frac{d\tau}{dy} = -\rho g \sin\alpha \tag{6-19}$$

and then apply the no-slip condition at $y = h$ and the *free-surface condition*, $\tau = 0$, at $y = 0$. What is the mean velocity in the layer? What is the thickness of a layer whose rate of flow down the incline (per unit width in the direction perpendicular to the plane in Figure 6-3) is Q?

6-3 ASTHENOSPHERIC COUNTERFLOW

One model for the flow in the mantle associated with the movement of the surface plates is a *counterflow* immediately beneath the lithosphere, as shown in Figure 6-4. The lithosphere is assumed to be a rigid plate of thickness h_L moving with velocity u_0. Beneath the lithosphere is an asthenosphere of thickness h and uniform viscosity μ. At the base of the asthenosphere we assume that the mantle is stationary; that is, $u = 0$. The boundary conditions $u = 0$ at $y = h$ and $u = u_0$ at $y = 0$ have been satisfied in writing Equation (6-12) so that this equation gives the flow in the asthenosphere. *Conservation of mass* requires that the flow of material in the $+x$ direction in the lithosphere must be balanced by a counterflow in the asthenosphere. For this model the net horizontal flow as illustrated in Figure 6-4 is zero. Quantitatively this can be written

$$u_0 h_L + \int_0^h u\, dy = 0 \tag{6-20}$$

where the first term is the *flux of material* in the lithosphere and the second term is the flux of material in the asthenosphere (per unit distance perpendicular to the Figure 6-4). By substituting Equation (6-12) into Equation (6-20) and integrating, we obtain

$$u_0 h_L - \frac{h^3}{12\mu}\frac{dp}{dx} + \frac{u_0 h}{2} = 0 \tag{6-21}$$

where dp/dx is the horizontal pressure gradient in the asthenosphere. We can solve Equation (6-21) for the pressure gradient that satisfies the counter-

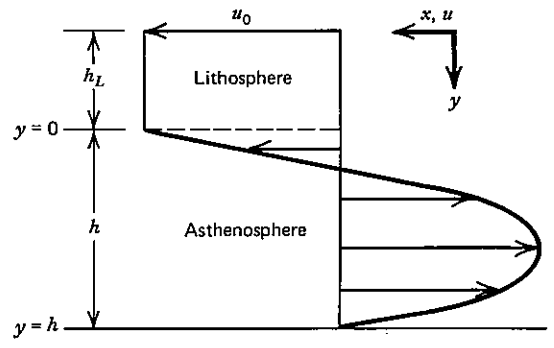

Figure 6-4 Velocity profile associated with the asthenospheric counterflow model.

flow condition

$$\frac{dp}{dx}=\frac{12\mu u_0}{h^2}\left(\frac{h_L}{h}+\frac{1}{2}\right) \qquad (6\text{-}22)$$

Substitution of this result into Equation (6-12) gives the velocity profile in the asthenosphere

$$u=u_0\left\{1-\frac{y}{h}+6\left(\frac{h_L}{h}+\frac{1}{2}\right)\left(\frac{y^2}{h^2}-\frac{y}{h}\right)\right\} \qquad (6\text{-}23)$$

This velocity profile is illustrated in Figure 6-4; it is independent of the viscosity.

The shear stress on the base of the lithosphere τ_{LA} due to the counterflow in the asthenosphere can be evaluated directly using Equations (6-1) and (6-23). The result is

$$\tau_{LA}=-\frac{2\mu u_0}{h}\left(2+3\frac{h_L}{h}\right) \qquad (6\text{-}24)$$

The minus sign in Equation (6-24) indicates that the asthenosphere exerts a drag force on the base of the lithosphere tending to oppose its motion. For $\mu=4\times10^{19}$ Pa s (a possible value for the viscosity of the asthenosphere), $h_L=100$ km, $h=200$ km, and $u_0=50$ mm yr^{-1}, we get 2.2 MPa (22 bars) for the magnitude of the shear stress on the base of the lithosphere from Equation (6-24).

The asthenospheric counterflow considered in this section requires that the pressure in the asthenosphere increase with x; that is, p must increase in the direction of *seafloor spreading*. This increase in pressure with distance from a ridge could only be provided by a *hydrostatic head* associated with topography; that is, the ocean floor would have to rise with distance from the ridge. The situation is sketched in Figure 6-5. The pressure in the asthenosphere a distance b beneath the ridge is given by the hydrostatic formula as

$$p=\rho_w g w+\rho g(w_r-w+b) \qquad (6\text{-}25)$$

where ρ_w is the density of seawater, w is the depth of the ocean a distance x from the ridge, ρ is the mantle density, and w_r is the depth of the ocean at the ridge. By differentiating equation (6-25) with respect to x, we can relate the slope of the seafloor to the horizontal pressure gradient in the asthenosphere

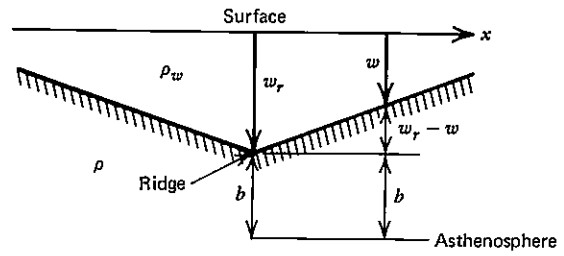

Figure 6-5 The asthenospheric counterflow model requires the seafloor to rise with distance from a ridge in order to supply the pressure required to drive the return flow toward the ridge in the asthenosphere.

$$\frac{dp}{dx}=-(\rho-\rho_w)g\frac{dw}{dx} \qquad (6\text{-}26)$$

A positive dp/dx requires a negative dw/dx or an ocean depth that decreases with x. By combining Equations (6-22) and (6-26), we can solve for the slope of the seafloor required by the asthenospheric counterflow model. We find

$$\frac{dw}{dx}=-\frac{12\mu u_0}{(\rho-\rho_w)gh^2}\left(\frac{h_L}{h}+\frac{1}{2}\right) \qquad (6\text{-}27)$$

For $\rho_w=1000$ kg m^{-3}, $\rho=3300$ kg m^{-3}, $g=10$ m s^{-2}, and the other parameter values given above, the slope of the seafloor is $dw/dx=-7.2\times10^{-4}$. Across the width of the Pacific Ocean, $x=10{,}000$ km, this would give a decrease in depth of 7.2 km. No systematic decrease in ocean depth as one moves to the northwest in the Pacific is observed.

The pressure gradient required to drive the asthenospheric counterflow would also result in a gravity anomaly. The value of the anomaly Δg can be obtained using the Bouguer gravity formula, Equation (5-111), which combined with Equation (6-27) gives

$$\frac{d(\Delta g)}{dx}=\frac{24\pi G\mu u_0}{gh^2}\left(\frac{h_L}{h}+\frac{1}{2}\right) \qquad (6\text{-}28)$$

For the example considered above we find that $d\Delta g/dx=10^{-10}$ s^{-2}. Across the width of the Pacific this gives a gravity anomaly of 7.2 mm s^{-2}, which is also not observed. The conclusion is that the shallow counterflow model for mantle convection is not correct and that significant convective flows occur to at least a depth of 700 km in the mantle.

Problem 6-5 For an asthenosphere with a viscosity $\mu=4\times10^{19}$ Pa s and a thickness $h=200$ km, what is the shear stress on the base of the lithosphere if there is no counterflow ($\partial p/\partial x=0$)? Assume $u_0=50$ mm yr^{-1} and that the base of the asthenosphere has zero velocity.

Problem 6-6 Assume that the base stress obtained in Problem 6-5 is acting on 6000 km of lithosphere with a thickness of 100 km. What tensional stress in the lithosphere ($h_L=100$ km) must be applied at a trench to overcome this basal drag?

6-4 PIPE FLOW

With subsequent applications to flows in aquifers and volcanic conduits in mind, we next consider viscous flow through a circular pipe. The pipe has a radius R and a length l, as illustrated in Figure 6-6. The flow is driven by the pressure difference (p_1-p_0) applied between the sections a distance l apart. We assume that the velocity of the fluid along the pipe u depends only on distance from the center of the pipe r. The form of the velocity profile $u(r)$ can be found by writing a force balance on a cylindrical *control volume* of radius r and length l, as shown in Figure 6-6. The net pressure force on the ends of the cylindrical control volume is $(p_1-p_0)\pi r^2$; this is a force along the cylinder axis in the direction of flow. Since there can be no net force on the control volume if the flow is *steady*, this pressure force must be balanced by the shear force acting on the cylindrical surface of the control volume. The shear stress on the cylindrical surface $\tau(r)$ exerts a net *frictional force* $-2\pi rl\tau(r)$ on the control volume (τ is a negative quantity). The force balance equation is thus

$$\pi r^2(p_1-p_0)=-2\pi rl\tau \qquad (6\text{-}29)$$

or

$$\tau=\frac{r}{2}\frac{dp}{dx} \qquad (6\text{-}30)$$

where dp/dx is the pressure gradient along the pipe—(Equation (6-7).

In the cylindrical geometry in Figure 6-6, the shear stress τ is directly proportional to the radial gradient of the velocity u

$$\tau=\mu\frac{du}{dr} \qquad (6\text{-}31)$$

As in Equation (6-1), the viscosity μ is the constant of proportionality. By substituting Equation (6-31) into Equation (6-30), we obtain an expression for the slope of the velocity profile,

$$\frac{du}{dr}=\frac{r}{2\mu}\frac{dp}{dx} \qquad (6\text{-}32)$$

which can be integrated to give

$$u=-\frac{1}{4\mu}\frac{dp}{dx}(R^2-r^2) \qquad (6\text{-}33)$$

We used the condition $u=0$ at $r=R$ in obtaining Equation (6-33). The velocity profile in the pipe is a parabaloid of revolution; it is known as *Poiseuille flow*.

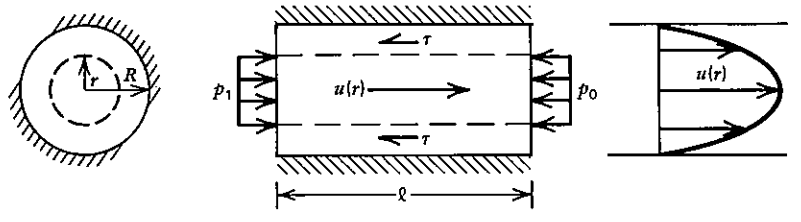

Figure 6-6 Poiseuille flow through a circular pipe.

The maximum velocity in the pipe u_{max} occurs at $r=0$. From Equation (6-33) it is given by

$$u_{max} = -\frac{R^2}{4\mu}\frac{dp}{dx} \tag{6-34}$$

Since dp/dx is negative when $p_1 > p_0$, u_{max} is a positive quantity. The *volumetric flow rate* Q through the pipe is the total volume of fluid passing a cross section per unit time. The flow through an annulus of thickness dr and radius r occurs at the rate $2\pi r\,dru(r)$; Q is the integral of this over a cross section

$$Q = \int_0^R 2\pi ru\,dr \tag{6-35}$$

Upon substituting Equation (6-33) into Equation (6-35) and carrying out the integration, we get

$$Q = -\frac{\pi R^4}{8\mu}\frac{dp}{dx} \tag{6-36}$$

If we divide Q by the cross-sectional area of the pipe πR^2, we obtain the mean velocity $\bar{u}$ in the pipe

$$\bar{u} = -\frac{R^2}{8\mu}\frac{dp}{dx} \tag{6-37}$$

By comparing Equations (6-34) and (6-37), we see that

$$\bar{u} = \frac{1}{2}u_{max} \tag{6-38}$$

The mean and maximum velocities in the pipe are directly proportional to the pressure gradient and inversely proportional to the viscosity. This result is valid as long as the flow is *laminar*.

It is often convenient in fluid mechanics to work in terms of *dimensionless variables*. The relation between the mean velocity in the pipe and the pressure gradient—Equation (6-37)—can be put into standard dimensionless form by introducing two quantities: a dimensionless pressure gradient or *friction factor* f and the *Reynolds number* Re. The friction factor is defined as

$$f \equiv \frac{-4R}{\rho\bar{u}^2}\frac{dp}{dx} \tag{6-39}$$

and the Reynolds number is given by

$$Re \equiv \frac{\rho\bar{u}D}{\mu} \tag{6-40}$$

where $D=2R$ is the pipe diameter. Using Equations (6-39) and (6-40), we can rewrite Equation (6-37) as

$$f = \frac{64}{Re} \tag{6-41}$$

The inverse dependence of the friction factor on the Reynolds number in laminar flow is shown in Figure 6-7.

At sufficiently high Reynolds numbers, observed pressure drops become considerably higher than those given by laminar theory. The flow in the pipe becomes unsteady with *random eddies*. This is known as *turbulent flow*. The qualitative difference between laminar and turbulent flows is illustrated in Figure 6-8. The principal advantage of the formulation of the problem in nondimensional form is that the *transition to turbulent flow* occurs at $Re \approx 2200$ independent of the pipe radius, flow velocity, or type of fluid considered (viscosity and density). The mean velocity corresponding to the transition Reynolds number of 2200 is 22 mm s^{-1} for water with a viscosity of 10^{-3} Pa s flowing in a 0.1 m diameter pipe. This illustrates that most flows of ordinary liquids and gases are in the turbulent regime.

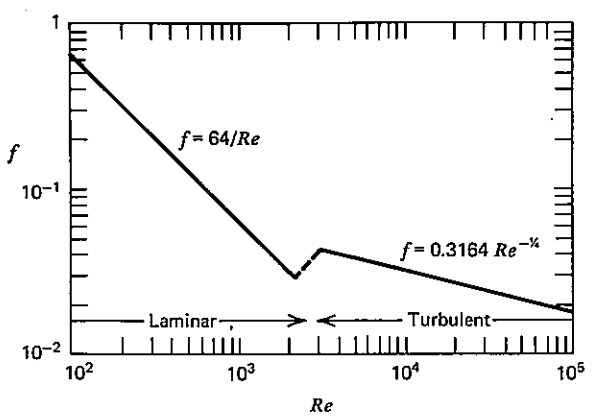

Figure 6-7 Dependence of the friction factor f on the Reynolds number Re for laminar flow, from Equation (6-41), and for turbulent flow, from Equation (6-42).

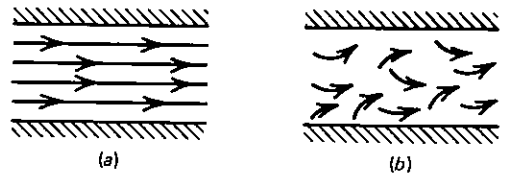

Figure 6-8 Illustration of the difference between (*a*) laminar and (*b*) turbulent flow. In laminar flow the flow is steady, and the fluid flows parallel to the walls: lateral transport of momentum takes place on a molecular scale. In turbulent flow the flow is unsteady, and there are many time-dependent eddies and swirls. These eddies are much more effective in the lateral transport of momentum than are molecular processes. Therefore, the friction factor (pressure drop) in turbulent flows is larger at a prescribed Reynolds number (flow velocity).

No theoretical equivalent to the Newtonian relationship between shear stress and rate of strain as given in Equation (6-1) or Equation (6-31) exists for turbulent flows. It is found empirically that

$$f = 0.3164Re^{-1/4} \tag{6-42}$$

in the turbulent flow regime. This result is also shown in Figure 6-7 along with the transition from laminar to turbulent flow.

Problem 6-7 Determine the Reynolds number for the asthenospheric flow considered in Problem 6-5. Base the Reynolds number on the thickness of the flowing layer and the mean velocity ($u_0 = 50$ mm yr^{-1} and $\rho = 3200$ kg m^{-3}). This problem illustrates that the viscosity of mantle rock is so high that the Reynolds number is generally small. Thus mantle flows are laminar.

6-5 ARTESIAN AQUIFER FLOWS

Naturally occurring springs are usually due to the flow of groundwater from a high elevation to a low elevation. The flow takes place through an aquifer or *permeable formation*. Figure 6-9 shows an idealized model of an aquifer in the shape of a semicircle of radius R', a form suggested by the geometry of porous layers in folded sedimentary

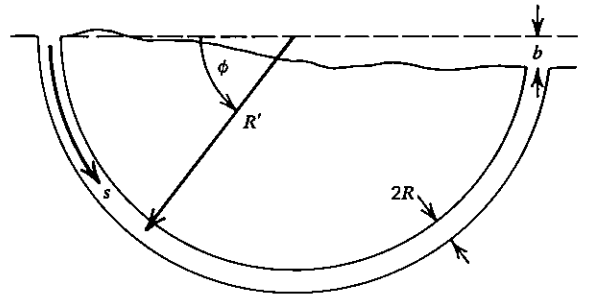

Figure 6-9 A semicircular aquifer with a circular cross section (a toroid). A hydrostatic head b is available to drive the flow.

rock. The entrance of the aquifer lies a distance b above the exit, and its cross section is assumed to be circular with radius R. The hydrostatic pressure head available to drive flow through the aquifer is ρgb, where ρ is the density of water. Since the overall length of the aquifer is $\pi R'$ ($R' \gg b$), the driving pressure gradient is

$$\frac{dp}{ds} = \frac{-\rho gb}{\pi R'} \tag{6-43}$$

where s is distance along the aquifer. The volumetric flow rate produced by this pressure gradient can be calculated from Equation (6-36) if the flow through the aquifer is laminar. The result of substituting Equation (6-43) into Equation (6-36), identifying dp/ds as dp/dx, is

$$Q = \frac{\rho gbR^4}{8\mu R'} \tag{6-44}$$

If the flow is turbulent, we can determine the resulting Q by using the empirical relation (6-42) between f and Re. The first step is to recast Equation (6-42) into dimensional form using the definitions of f and Re. We find

$$\frac{-4R}{\rho\bar{u}^2}\frac{dp}{dx} = 0.3164\left(\frac{\mu}{\rho\bar{u}2R}\right)^{1/4} \tag{6-45}$$

The result of rearranging Equation (6-45) so as to determine $\bar{u}$ is

$$\bar{u} = \left(\frac{4\times 2^{1/4}}{0.3164}\right)^{4/7}\left(-\frac{1}{\rho}\frac{dp}{dx}\right)^{4/7}R^{5/7}\left(\frac{\rho}{\mu}\right)^{1/7} \tag{6-46}$$

Since Q is $\pi R^2 \bar{u}$, we obtain the volumetric flow rate through the aquifer for turbulent flow by multiplying Equation (6-46) by πR^2 and substituting for $(-1/\rho)(dp/dx)$ from Equation (6-43). One finds

$$Q = 7.686\left(\frac{gb}{R'}\right)^{4/7}\left(\frac{\rho}{\mu}\right)^{1/7} R^{19/7} \qquad (6\text{-}47)$$

Problem 6-8 A spring has a flow of 100 liters per minute. The entrance to the spring lies 2 km away from the outlet and 50 m above it. If the aquifer supplying the spring is modeled according to Figure 6-9, find its cross-sectional radius. What is the average velocity? Is the flow laminar or turbulent?

6-6 FLOW THROUGH VOLCANIC PIPES

Another example of naturally occurring pipe flow is the flow of magma through volcanic conduits of nearly circular cross section. The upward flow of the magma is driven by the natural buoyancy of the lighter magma relative to the denser surrounding rock. At a depth h the *lithostatic pressure* in the rock is $\rho_s g h$, where ρ_s is the rock density. At the same depth the *hydrostatic pressure* in a stationary column of magma is $\rho_l g h$, where ρ_l is the magma density. Assuming that the lithostatic and hydrostatic pressures are equal in the pipe, the pressure gradient available to drive the magma up to the surface is $-(\rho_s - \rho_l)g$. The assumption of equal lithostatic and hydrostatic pressures in the pipe is equivalent to assuming that the walls of the pipe are free to deform as the magma is driven upward. The volumetric flow Q driven by the above pressure gradient through a volcanic pipe of radius R is, from Equation (6-36),

$$Q = \frac{\pi}{8}\frac{(\rho_s - \rho_l)gR^4}{\mu} \qquad (6\text{-}48)$$

if the flow is laminar. From Equation (6-46) and $Q = \pi R^2 \bar{u}$, the volumetric flow for turbulent conditions is

$$Q = 14.8\frac{R^{19/7}[(\rho_s - \rho_l)g]^{4/7}}{\rho_l^{3/7}\mu^{1/7}} \qquad (6\text{-}49)$$

Problem 6-9 Determine the rate at which magma flows up a two-dimensional channel of width d under the buoyant pressure gradient $-(\rho_s - \rho_l)g$. Assume laminar flow.

6-7 CONSERVATION OF FLUID IN TWO DIMENSIONS

We now extend our studies of viscous fluid flow to two dimensions. We consider a general flow in the xy plane with the corresponding *velocity components* u and v. The spatial variations of these two velocity components are constrained by the need to conserve fluid. We consider a rectangular control volume with dimensions δx and δy, as illustrated in Figure 6-10. The flow rate per unit area in the x direction at x is u. The flow rate per unit area at $x + \delta x$ is

$$u(x + \delta x) = u + \frac{\partial u}{\partial x}\delta x \qquad (6\text{-}50)$$

The net flow rate out of the region between x and $x + \delta x$ per unit area normal to the x direction is

$$u + \frac{\partial u}{\partial x}\delta x - u = \frac{\partial u}{\partial x}\delta x \qquad (6\text{-}51)$$

Similarly, flow in the y direction (vertically downward) yields a net volume flow per unit area normal to the y direction out of the region between y and $y + \delta y$ given by

$$v + \frac{\partial v}{\partial y}\delta y - v = \frac{\partial v}{\partial y}\delta y \qquad (6\text{-}52)$$

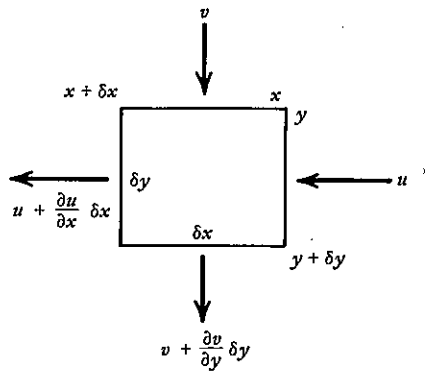

Figure 6-10 Flow across the surfaces of an infinitesimal rectangular element.

To find the net rate at which fluid flows out of the rectangular region shown in Figure 6-10, we must combine the flows in the two directions. The net outward flow rate in the x direction is $(\partial u/\partial x)\delta x$ times the area of the face across which the flow occurs, which is δy multiplied by a unit dimension in the direction normal to the diagram. The net outward flow rate in the x direction is thus $(\partial u/\partial x)\delta x \delta y$. Similarly the net outward flow rate in the y direction is $(\partial v/\partial y)\delta y \delta x$. The total net outward flow rate per unit area of the rectangle is

$$\frac{\partial u}{\partial x} + \frac{\partial v}{\partial y}$$

If the flow is steady (time-independent), and there are no density variations to consider, there can be no net flow into or out of the rectangle. The *conservation of fluid* or *continuity equation* is

$$\frac{\partial u}{\partial x} + \frac{\partial v}{\partial y} = 0 \qquad (6\text{-}53)$$

This is the form of the continuity equation appropriate to an *incompressible fluid*.

6-8 ELEMENTAL FORCE BALANCE IN TWO DIMENSIONS

The forces acting on the control volume in Figure 6-10 must be in balance. Included in the force balance are the pressure forces, *viscous forces*, and *gravity force*. We neglect the *inertial force* associated with the *acceleration* of a fluid element. This is appropriate for the slow motion of very viscous or high Prandtl number fluids. The earth's mantle behaves as a highly viscous fluid on geologic time scales. The viscosity of the mantle is about 10^{21} Pa s (10^{22} poise); its density and thermal diffusivity are about 4000 kg m^{-3} (4 g cm^{-3}) and 1 mm^2 s^{-1} (10^{-2} cm^2 s^{-1}). Thus the Prandtl number of the earth's mantle is about 10^{23}. The balance of pressure, viscous, and gravity forces and the neglect of inertial forces are equivalent to the application of *Newton's second law of motion* to a fluid element with the neglect of its acceleration. It is also equivalent to a statement of momentum conservation.

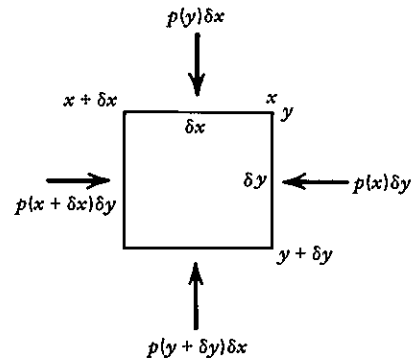

Figure 6-11 Pressure forces acting on an infinitesimal rectangular fluid element.

The pressure forces acting on an infinitesimal rectangular element of fluid are illustrated in Figure 6-11. Since pressure is force per unit area, $p\,\delta y$ (times a unit length in the direction normal to the plane of the figure) is the force acting to the left on the face of the rectangle located at x, for example. Pressure forces act perpendicular to surfaces and are directed into the volume enclosed by the surface. The net pressure force on the element in the x direction per unit area of the fluid element is

$$\frac{p(x)\delta y - p(x + \delta x)\delta y}{\delta x \delta y} = -\frac{[p(x + \delta x) - p(x)]}{\delta x} \qquad (6\text{-}54)$$

which by virtue of a simple Taylor series expansion is

$$-\frac{\partial p}{\partial x}$$

Thus, only if there is a pressure gradient in the x direction will there be any net pressure force on the fluid element. If there is no such pressure variation, the pressure forces on opposite sides of the element will simply cancel each other and there will be no net effect. Similarly, the net pressure force on the element in the y direction per unit area of the element is

$$-\frac{\partial p}{\partial y}$$

of the fluid. Show by dimensional analysis that

$$\frac{D}{\rho U^2 a^2} = f\left(\frac{\rho U a}{\mu}\right) \tag{6-232}$$

where f is an arbitrary function. Since the equations of slow viscous flow are linear, D can only be directly proportional to U. Use this fact together with Equation (6-232) to conclude that

$$D \propto \mu U a \tag{6-233}$$

Problem 6-23 Consider a spherical bubble of a low-viscosity fluid with density ρ_b rising or falling through a much more viscous fluid with density ρ_f and viscosity μ_f because of a buoyancy force. For this problem the appropriate boundary conditions at the surface of the sphere, $r = a$, are

$$u_r = 0, \tau_{r\theta} = 0 \quad \text{at} \quad r = a$$

Using Equations (6-210), (6-211), and (6-220) show that

$$u_r = U\left(-1 + \frac{a}{r}\right)\cos\theta \tag{6-234}$$

$$u_\theta = U\left(1 - \frac{1}{2}\frac{a}{r}\right)\sin\theta \tag{6-235}$$

By integrating Equation (6-196), show that on $r = a$

$$p = \frac{\mu_f U}{a}\cos\theta \tag{6-236}$$

The drag force is obtained by carrying out the integral

$$D = 2\pi a^2 \int_0^\pi \left(p - 2\mu_f \frac{\partial u_r}{\partial r}\right)_{r=a} \cos\theta \sin\theta \, d\theta \tag{6-237}$$

Show that

$$D = 4\pi\mu_f a U \tag{6-238}$$

and demonstrate that the terminal velocity of the bubble in the fluid is

$$U = \frac{a^2 g(\rho_f - \rho_b)}{3\mu_f} \tag{6-239}$$

6-15 PIPE FLOW WITH HEAT ADDITION

We now turn to problems involving both fluid flow and heat transfer. As our first example we treat the flow in a pipe with heat addition or heat loss, a situation relevant to the heating of water in an aquifer. We consider the heat balance on a thin cylindrical shell of fluid in the pipe. The thickness of the shell is δr, and its length is δx, as illustrated in Figure 6-33. The heat conducted out of the cylindrical surface at $r + \delta r$ per unit time is

$$2\pi(r + \delta r)\,\delta x q_r(r + \delta r)$$

where $q_r(r + \delta r)$ is the radial *heat flux* at $r + \delta r$. The heat conducted into the shell across its inner cylindrical surface is

$$2\pi r\,\delta x q_r(r)$$

per unit time. Since δr is small, we can expand $q_r(r + \delta r)$ as

$$q_r(r + \delta r) = q_r(r) + \frac{\partial q_r}{\partial r}\delta r + \cdots$$

By neglecting higher powers of δr, we can write the net rate at which heat is conducted into the cylindrical shell through its inner and outer surfaces as

$$2\pi\,\delta x[r q_r(r) - (r + \delta r) q_r(r + \delta r)] = -2\pi\,\delta x\left(r\frac{\partial q_r}{\partial r} + q_r\right)\delta r \tag{6-240}$$

In cylindrical coordinates, the radial heat flux q_r is related to the radial temperature gradient $\partial T/\partial r$ by Fourier's law of heat conduction—see

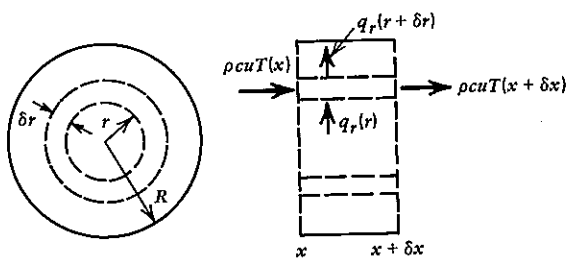

Figure 6-33 Heat balance on a small cylindrical shell in a circular pipe.

Problem 4-21,

$$q_r = -k\frac{\partial T}{\partial r} \tag{6-241}$$

where k is the thermal conductivity of the fluid. Expression (6-240) for the net effect of radial heat conduction can thus be rewritten in terms of the temperature as

$$2\pi\,\delta x\,\delta r k\left(r\frac{\partial^2 T}{\partial r^2} + \frac{\partial T}{\partial r}\right)$$

The amount of heat convected out of the shell at $x + \delta x$ by the velocity $u(r)$ per unit time is given by

$$2\pi r\,\delta r u \rho c T(x + \delta x)$$

and the amount of heat convected into the shell at x per unit time is given by

$$2\pi r\,\delta r u \rho c T(x)$$

By using the first two terms of a Taylor series expansion for $T(x + \delta x)$, we find that the net rate at which fluid carries heat out of the shell is

$$2\pi r\,\delta r u \rho c[T(x + \delta x) - T(x)] = 2\pi r\,\delta r u \rho c\frac{\partial T}{\partial x}\delta x \tag{6-242}$$

If the flow is steady so that the temperature of the fluid does not change with time and if axial heat conduction is unimportant compared with advection of heat by the flow, the net effects of radial heat conduction and axial heat advection must balance. Therefore we can equate the right side of Equation (6-242) with the modified form of the right side of Equation (6-240) to obtain

$$\rho u c\frac{\partial T}{\partial x} = k\left(\frac{\partial^2 T}{\partial r^2} + \frac{1}{r}\frac{\partial T}{\partial r}\right) \tag{6-243}$$

By equating axial heat advection to radial heat conduction, we also tacitly assumed that *viscous dissipation* or *frictional heating* in the fluid is negligible.

We can determine the temperature distribution in the pipe using Equation (6-243) for the laminar flow considered in Section 6-4. The velocity as a function of radius can be expressed in terms of the mean velocity $\bar{u}$ by combining Equations (6-33) and (6-37) to give

$$u = 2\bar{u}\left[1 - \left(\frac{r}{R}\right)^2\right] \tag{6-244}$$

We consider the case in which the wall temperature of the pipe T_w is changing linearly along its length; that is,

$$T_w = C_1 x + C_2 \tag{6-245}$$

where C_1 and C_2 are constants. Accordingly, we assume that the temperature of the fluid is given by

$$T = C_1 x + C_2 + \theta(r) = T_w + \theta(r) \tag{6-246}$$

(In this situation, the net contribution of axial heat conduction to the heat balance of a small cylindrical shell vanishes identically.) Thus θ is the difference between the fluid temperature and the wall temperature. Substitution of Equations (6-244) and (6-246) into Equation (6-243) yields

$$2\rho c\bar{u}\left[1 - \left(\frac{r}{R}\right)^2\right]C_1 = k\left(\frac{d^2\theta}{dr^2} + \frac{1}{r}\frac{d\theta}{dr}\right) \tag{6-247}$$

The boundary conditions are

$$T = T_w \quad \text{at} \quad r = R \tag{6-248}$$

and

$$q_r = 0 \quad \text{at} \quad r = 0 \tag{6-249}$$

The latter condition is required because there is no line source or sink of heat along the axis of the pipe. Condition (6-248) is satisfied if

$$\theta_{r=R} = 0 \tag{6-250}$$

and condition (6-249), with the aid of Fourier's law (6-241), becomes

$$\left(\frac{d\theta}{dr}\right)_{r=0} = 0 \tag{6-251}$$

The solution of Equation (6-247) that satisfies these boundary conditions is

$$\theta = -\frac{\rho c\bar{u}C_1 R^2}{8k}\left\{3 - 4\frac{r^2}{R^2} + \frac{r^4}{R^4}\right\} \tag{6-252}$$

The heat flux to the wall q_w can be found by substituting Equation (6-252) into Fourier's law—

Equation (6-241)—and evaluating the result at $r=R$. One finds

$$q_w=-\tfrac{1}{2}\rho c\bar{u}RC_1 \qquad (6\text{-}253)$$

The heat flux is thus a constant, independent of x. If C_1 is positive, the wall temperature increases in the direction of flow, and heat flows through the wall of the pipe into the fluid. If C_1 is negative, the wall temperature decreases in the direction of flow, and heat flows out of the fluid into the wall of the pipe. The heat flux to the wall can be expressed in a convenient way by introducing a *heat transfer coefficient* h between the wall heat flux and the excess fluid temperature according to

$$q_w=h(\bar{T}-T_w)=h\bar{\theta} \qquad (6\text{-}254)$$

where the overbar represents an average over the cross section of the pipe. The average is weighted by the flow per unit area, that is, the velocity through an annular area at radius r. Thus the flow-weighted average excess fluid temperature is

$$\bar{\theta}=\frac{2\pi\int_0^R\theta ur\,dr}{\pi R^2\bar{u}}=\frac{-11\rho c\bar{u}C_1R^2}{48k} \qquad (6\text{-}255)$$

By combining Equations (6-253) to (6-255), we find that the heat transfer coefficient for laminar flow in a circular pipe is

$$h=\frac{48k}{11D} \qquad (6\text{-}256)$$

where $D=2R$ is the pipe diameter. Equation (6-256) is valid only for Reynolds numbers less than about 2200. At higher values of the Reynolds number the flow is turbulent.

It is common in the fluid mechanics literature to introduce a dimensionless measure of the heat transfer coefficient. This is known as the *Nusselt number Nu*, which, for pipe flow with heat addition, is defined as

$$Nu\equiv\frac{hD}{k}=\frac{48}{11}=4.36 \qquad (6\text{-}257)$$

The Nusselt number measures the efficiency of the heat transfer process. If the temperature difference $\bar{T}-T_w$ were established across a stationary layer of fluid of thickness D and thermal conductivity k, the conductive heat flux q_c would be

$$q_c=\frac{k(\bar{T}-T_w)}{D}=\frac{q_wk}{Dh} \qquad (6\text{-}258)$$

Thus the Nusselt number can be written

$$Nu=\frac{q_w}{q_c} \qquad (6\text{-}259)$$

and heat transfer with fluid flow through the pipe is 4.36 times more efficient than conductive heat transport through an equivalent stationary fluid layer across which the same temperature difference is applied.

Problem 6-24 Consider unidirectional flow driven by a constant horizontal pressure gradient through a channel with stationary plane parallel walls, as discussed in Section 6-2. Determine the temperature distribution in the channel, the wall heat flux, the heat transfer coefficient, and the Nusselt number by assuming, as in the pipe flow problem above, that the temperature of both walls and the fluid varies linearly with distance x along the channel. You will need the form of the temperature equation in two dimensions which balances horizontal heat advection against vertical heat conduction. This has been given in Equation (4-149).

6-16 AQUIFER MODEL FOR HOT SPRINGS

The results of the previous section can be used to study the heating of water flowing through an aquifer surrounded by hot rocks. We again consider the semicircular aquifer with circular cross section illustrated in Figure 6-9. If we balance the heat convected along the aquifer against the heat lost or gained by conduction to the walls, we can write

$$\pi R^2\rho c\bar{u}\frac{d\bar{T}}{ds}=2\pi Rh(T_w-\bar{T}) \qquad (6\text{-}260)$$

where s is the distance measured along the aquifer from the entrance, $\bar{u}$ is the mean velocity in the aquifer, $\bar{T}$ is the flow-averaged temperature of the aquifer fluid, and T_w is the temperature of the aquifer wall rock. We assume laminar flow so that

the heat transfer coefficient h is given by Equation (6-256). The coordinate s can be related to the angle ϕ (see Figure 6-9) by

$$s=R'\phi \qquad (6\text{-}261)$$

We assume that the wall temperature of the aquifer can be related to the local geothermal gradient β by

$$T_w=R'\beta\sin\phi+T_0 \qquad (6\text{-}262)$$

where T_0 is the surface temperature and β is taken to be constant. Equation (6-262) assumes that the flow in the aquifer does not affect the temperature of the adjacent rock. Substitution of Equations (6-256), (6-261), and (6-262) into Equation (6-260) yields

$$\frac{R^2\rho c\bar{u}}{R'}\frac{d\bar{T}}{d\phi}=\frac{48}{11}k(R'\beta\sin\phi+T_0-\bar{T}) \qquad (6\text{-}263)$$

This equation can be simplified through the introduction of the *Péclet number Pe* defined by

$$Pe=\frac{\rho c\bar{u}R}{k} \qquad (6\text{-}264)$$

The Péclet number is a dimensionless measure of the mean velocity of the flow through the aquifer. It is related to the dimensionless parameters *Re* and *Pr* already introduced. Since the thermal diffusivity κ is $k/\rho c$, *Pe* can be written as

$$Pe=\frac{\bar{u}R}{\kappa} \qquad (6\text{-}265)$$

Using the definitions of the Reynolds number *Re* —Equation (6-40)—and the Prandtl number *Pr*—Equation (6-3)—we can further rewrite Equation (6-265) as

$$Pe=\frac{1}{2}\frac{\bar{u}2R}{\nu}\frac{\nu}{\kappa}=\frac{1}{2}RePr \qquad (6\text{-}266)$$

The simplification of Equation (6-263) is also facilitated by the introduction of a dimensionless temperature θ defined by

$$\theta=\frac{\bar{T}-T_0}{\beta R'} \qquad (6\text{-}267)$$

With Equations (6-264) and (6-267) we can put Equation (6-263) into the form

$$\frac{11}{48}\frac{R}{R'}Pe\frac{d\theta}{d\phi}+\theta=\sin\phi \qquad (6\text{-}268)$$

This is a linear first-order differential equation that can be integrated using an *integrating factor*. With the boundary condition that the water entering the aquifer is at the surface temperature, $\bar{T}=T_0$ or $\theta=0$ at $\phi=0$, the solution can be written

$$\theta=\left[\frac{48R'}{11RPe}\sin\phi-\cos\phi+\exp\left(-\frac{48}{11}\frac{R'}{RPe}\phi\right)\right]\times\left(\frac{48}{11}\frac{R'}{RPe}\right)\left[1+\left(\frac{48R'}{11RPe}\right)^2\right]^{-1} \qquad (6\text{-}269)$$

The nondimensional temperature θ_e at the exit of the aquifer, $\phi=\pi$, is given by

$$\theta_e=\frac{\left[\exp\left(-\frac{48}{11}\frac{R'\pi}{RPe}\right)+1\right]\frac{48}{11}\frac{R'}{RPe}}{1+\left(\frac{48R'}{11RPe}\right)^2} \qquad (6\text{-}270)$$

The nondimensional exit temperature is plotted as a function of RPe/R' in Figure 6-34. It is seen that the exit temperature of the *hot spring* is a maximum for $RPe/R'=5$. Thus, for given values of all parameters other than $\bar{u}$, there is a particular flow rate through the aquifer that maximizes the exit temperature of the water. The maximum exit temperature is about one-half of the maximum wall temperature at the base of the aquifer, since

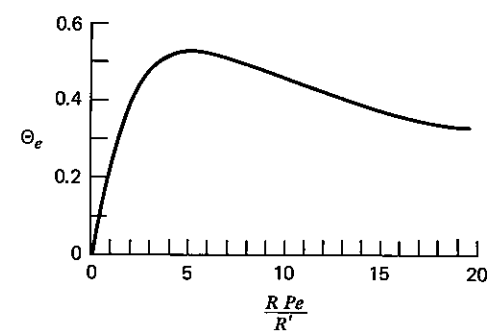

Figure 6-34 Dependence of the nondimensional temperature at the exit of the hot spring on the nondimensional flow rate through the aquifer.

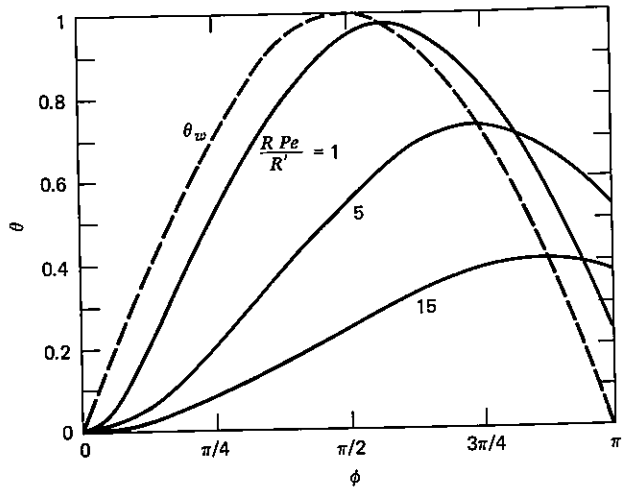

Figure 6-35 Dimensionless mean water temperature in the aquifer as a function of position for three nondimensional flow rates. The dashed line is the dimensionless aquifer wall temperature.

$\theta_e = 1/2$ corresponds to $\overline{T}_e = T_0 + \frac{1}{2}\beta R'$, and T_w at $\phi = \pi/2$ is $T_0 + \beta R'$ ($T_0 \ll \beta R'$).

In order to better understand why there is a maximum exit temperature, we show the mean temperature of the water in the aquifer as a function of position in Figure 6-35 for three flow rates. The dimensionless wall or rock temperature θ_w,

$$\theta_w = \frac{T_w - T_0}{\beta R'} \tag{6-271}$$

is also given in the figure. For a low flow rate, $RPe/R' = 1$, for example, the water temperature follows the wall temperature because of the large heat transfer, and the exit temperature is low. For very slow flow, $RPe/R' \to 0$, the water temperature equals the wall temperature $\theta = \theta_w = \sin\phi$, the exit temperature equals the entrance temperature, and there is no hot spring. For a high flow rate, $RPe/R' = 15$, for example, there is very little heat transfer, and the water does not heat up. In the limit $RPe/R' \to \infty$ the water temperature everywhere in the aquifer equals the entrance temperature, and there is no hot spring. The case of maximum exit temperature, $RPe/R' = 5$ and $\theta_e = 0.52$ is also shown in Figure 6-35.

Although the analysis given here has been greatly simplified, the results are applicable to the more general problem in which the temperature distribution in the rock through which the aquifer passes must also be determined. This requires a solution of Laplace's equation. Also, the transition to turbulence must be considered. The more complete solutions require numerical methods. However, the results show that the maximum temperature that can be expected from a hot spring is about one-half the temperature obtained by extrapolating the regional geothermal gradient to the base of the aquifer, similar to the result obtained here.

Problem 6-25 Verify by direct substitution that Equation (6-269) is the solution of Equation (6-268).

Problem 6-26 The results of this section were based on the assumption of a laminar heat transfer coefficient for the aquifer flow. Since this requires $Re < 2200$, what limitation is placed on the Péclet number?

6-17 THERMAL CONVECTION

As discussed in Section 1-13, plate tectonics is a consequence of thermal convection in the mantle driven largely by radiogenic heat sources and the cooling of the earth. When a fluid is heated, its density generally decreases because of thermal expansion. A fluid layer that is heated from below or from within and cooled from above has dense cool fluid near the upper boundary and hot light fluid at depth. This situation is gravitationally unstable, and the cool fluid tends to sink and the hot fluid tends to rise. This is thermal convection. The phenomenon is illustrated in Figure 1-59.

Appropriate forms of the continuity, force balance, and temperature equations for two-dimensional flow are required for a quantitative study of thermal convection. Density variations caused by thermal expansion lead to the buoyancy forces that drive thermal convection. Thus it is essential to account for density variations in the gravitational body force term of the conservation of momentum or force balance equation. In all other respects, however, the density variations are sufficiently small so that they can be neglected. This is known as the *Boussinesq approximation*. It allows us to use the incompressible conservation of fluid equation (6-53). The force balance equations (6-64) and (6-65) are also applicable. However, to account for the buoyancy forces, we must allow for small density variations in the vertical force balance, Equation (6-65), by letting

$$\rho = \rho_0 + \rho' \tag{6-272}$$

where ρ_0 is a reference density and $\rho' \ll \rho_0$. Equation (6-65) can then be written

$$0 = -\frac{\partial p}{\partial y} + \rho_0 g + \rho' g + \mu\left(\frac{\partial^2 v}{\partial x^2} + \frac{\partial^2 v}{\partial y^2}\right) \tag{6-273}$$

We can eliminate the hydrostatic pressure corresponding to the reference density by introducing

$$P = p - \rho_0 g y \tag{6-274}$$

as in Equation (6-66). The horizontal and vertical equations of motion, Equations (6-64) and (6-273), become

$$0 = -\frac{\partial P}{\partial x} + \mu\left(\frac{\partial^2 u}{\partial x^2} + \frac{\partial^2 u}{\partial y^2}\right) \tag{6-275}$$

$$0 = -\frac{\partial P}{\partial y} + \rho' g + \mu\left(\frac{\partial^2 v}{\partial x^2} + \frac{\partial^2 v}{\partial y^2}\right) \tag{6-276}$$

Density variations caused by temperature changes are given by Equation (4-172)

$$\rho' = -\rho_0 \alpha_v (T - T_0) \tag{6-277}$$

where α_v is the volumetric coefficient of thermal expansion and T_0 is the reference temperature corresponding to the reference density ρ_0. Substitution of Equation (6-277) into Equation (6-276) gives

$$0 = -\frac{\partial P}{\partial y} + \mu\left(\frac{\partial^2 v}{\partial x^2} + \frac{\partial^2 v}{\partial y^2}\right) - g\rho_0\alpha_v(T - T_0) \tag{6-278}$$

The last term in Equation (6-278) is the buoyancy force per unit volume. The gravitational buoyancy term depends on temperature. Thus the velocity field cannot be determined without simultaneously solving for the temperature field. Therefore we require the heat equation that governs the variation of temperature.

The energy balance must take account of heat transport by both conduction and convection. Consider the small two-dimensional element shown in Figure 6-36. Since the thermal energy content of the fluid is ρcT per unit volume, an amount of heat $\rho cTu\,\delta y$ is transported across the right side of the element by the velocity component u in the x direction. This is an energy flow per unit time and per unit depth or distance in the dimension perpendicular to the figure. If ρcTu is the energy flux at x, then $\rho cTu + \partial/\partial x(\rho cTu)\,\delta x$ is the energy flow rate per unit area at $x + \delta x$. The net

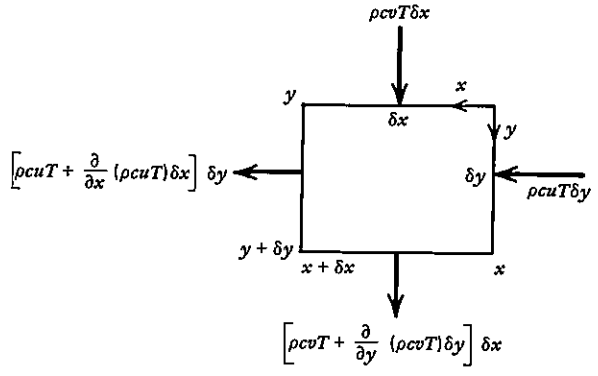

Figure 6-36 Heat transport across the surfaces of an infinitesimal rectangular element by convection.